



**Measurement of the shape of the boson transverse momentum distribution in
 $p\bar{p} \rightarrow Z/\gamma^* \rightarrow e^+e^- + X$ events produced at \sqrt{s} of 1.96 TeV**

The DØ Collaboration
URL <http://www-d0.fnal.gov>
(Dated: August 8, 2007)

We present a measurement of the shape of the Z -boson transverse momentum distribution in $p\bar{p} \rightarrow Z/\gamma^* \rightarrow e^+e^- + X$ events at a center-of-mass energy of 1.96 TeV using 0.98 fb^{-1} of data collected at the Fermilab Tevatron collider with the DØ detector. The measurement is made for events with electron-positron pairs with invariant mass $40 < M_{ee} < 200 \text{ GeV}/c^2$, Z boson transverse momenta $0 < q_T < 260 \text{ GeV}/c$, and Z boson rapidities $|y| < 3$. This represents the highest center-of-mass energy measurement of this quantity over the largest phase space available to date. Data is found to be consistent with predictions of perturbative quantum chromodynamics (pQCD) augmented by Collins-Soper-Sterman (CSS) resummation contributions at low q_T . Data at high q_T agree better with next-to-next-to leading order (NNLO) pQCD prediction than next-to leading order (NLO) predictions. Using events with $q_T < 30 \text{ GeV}$, g_2 , one of the phenomenological parameters used in Ladinsky-Yuan's parameterization of the CSS model, is determined to be $0.77 \pm 0.06 \text{ GeV}^2$. Data at large $|y|$ are compared with the prediction of CSS resummation and with alternative models that employ a resummed form factor with modifications in the small Bjorken x region of the proton wave function.

I. INTRODUCTION

A complete understanding of weak vector boson production is essential for maximizing the sensitivity to new physics at hadron colliders through the precision measurements of the W -boson mass, detailed studies of top quark production, and searches for production of the Higgs boson and other objects hypothesized to explain the mechanism of electroweak symmetry breaking. Studies of the Z boson play a particularly valuable role in that its kinematics can be precisely determined through measurement of its leptonic decays. Furthermore these modes can be observed with very small backgrounds. The phenomenology used to describe Z boson production is applicable to essentially all Drell-Yan type processes.

In addition, Z boson production serves as an ideal testing ground for predictions of quantum chromodynamics (QCD), since the bosons' transverse momentum, q_T , can be measured over a wide range of values and can be correlated with its rapidity. At high q_T (approximately greater than 20 GeV/ c), the radiation of a single parton with large transverse momentum dominates the cross section, and one expects predictions of fixed-order perturbative QCD [1], now available at NNLO [2], to yield reliable predictions. At lower q_T , multiple soft gluon emission can not be neglected, and the simple fixed-order perturbation calculation no longer gives accurate results. A soft gluon resummation technique developed by Collins, Soper, and Sterman (CSS) [3] gives reliable QCD predictions. A prescription [4] has been proposed for matching the low and high q_T regions in order to provide a continuous prediction for all q_T . The CSS resummation formalism allows the inclusion of contributions from large logarithms of the form $\ln^n(q_T/Q)$, where Q represents the four-momentum transfer arising from unsuppressed soft and collinear gluon radiation, to all orders of perturbation theory in an effective resummed form factor in impact-parameter (b) space or in transverse momentum space. In the case of b -space resummations, this form factor can be parameterized with the following form [5]:

$$S_{NP}(b, Q^2) = g_1 b^2 + g_2 b^2 \ln\left(\frac{Q^2}{Q_0^2}\right) + g_1 g_3 b \ln(100x_i x_j) \quad (1)$$

where x_i and x_j are the fractions of the incident hadron momenta carried by the colliding partons, Q_0 is a scale typical of the onset of non-perturbative effects, and g_1 , g_2 and g_3 are the phenomenological non-perturbative parameters that must be obtained from fits to the data. For measurements at the Fermilab Tevatron, the calculation is most sensitive to the value of g_2 and quite insensitive to the value of g_3 . Thus a measurement of the Z boson q_T spectrum can be used to test this formalism and to determine the value of g_2 . The resulting parameterization can be used to further reduce uncertainties in the W mass measurement due to uncertainties in the phenomenology of vector boson production [6].

Recent studies of data from deep inelastic scattering (DIS) experiments [7][8] indicate that the resummed form factor in the above equation may need to be modified for processes involving small-Bjorken- x parton in the initial state. In Ref. [9], the authors discuss how such a modification would influence the q_T distributions of vector and Higgs bosons produced in hadronic collisions. A wider transverse momentum distribution is predicted for Z bosons with very high rapidity (called "small- x broadening"). Z bosons produced with rapidities between 2 and 3 probe processes involving a parton with Bjorken- x between 0.002 and 0.006, and can be used as a test of the modified resummed form factor at small x .

Z boson q_T distributions have been published previously by the CDF [10] and DØ [11] collaborations using about 100 pb $^{-1}$ of data. In this paper, we report a new measurement with larger statistics and improved precision relative to these previous measurements. This measurement is also the first to present a q_T distribution for forward-rapidity Z bosons. A more detailed description of this analysis can be found in [12].

II. DØ DETECTOR AND EVENT SELECTION

The data sample used in this analysis was collected with the DØ detector at the Fermilab Tevatron collider at a center-of-mass energy of 1.96 TeV; the integrated luminosity is 980 ± 59 pb $^{-1}$ [13]. The DØ detector is described in more detail elsewhere [14]. It includes a central tracking system, composed of a silicon microstrip tracker (SMT) and a central fiber tracker (CFT), both located within a 2 T superconducting solenoidal magnet and optimized for tracking and vertexing capability at pseudorapidities of $|\eta| < 3$ and $|\eta| < 2.5$ respectively ($\eta = -\ln \tan(\theta/2)$, where θ is the polar angle with respect to the proton direction). Three liquid argon and uranium calorimeters provide coverage out to $|\eta| \approx 4.2$: a central section (CC) covering $|\eta|$ up to ≈ 1.1 , and two endcap calorimeters (EC) with an approximate coverage of $1.5 < |\eta| < 4.2$ for jets and $1.5 < |\eta| < 3.2$ for electrons. A muon system resides outside the calorimetry, and consists of tracking detectors, scintillation counters, and a 1.8 T toroid with coverage for $|\eta| < 2$. Luminosity is measured using scintillator arrays located in front of the endcap calorimeter, covering $2.7 < |\eta| < 4.4$. Trigger and data acquisition systems are designed to accommodate the high instantaneous luminosities of the Run II Tevatron.

Our selection criteria for candidate Z bosons require two isolated electromagnetic (EM) clusters away from the module boundaries of the calorimeters, that have shower shape consistent with that of an electron. At least one of

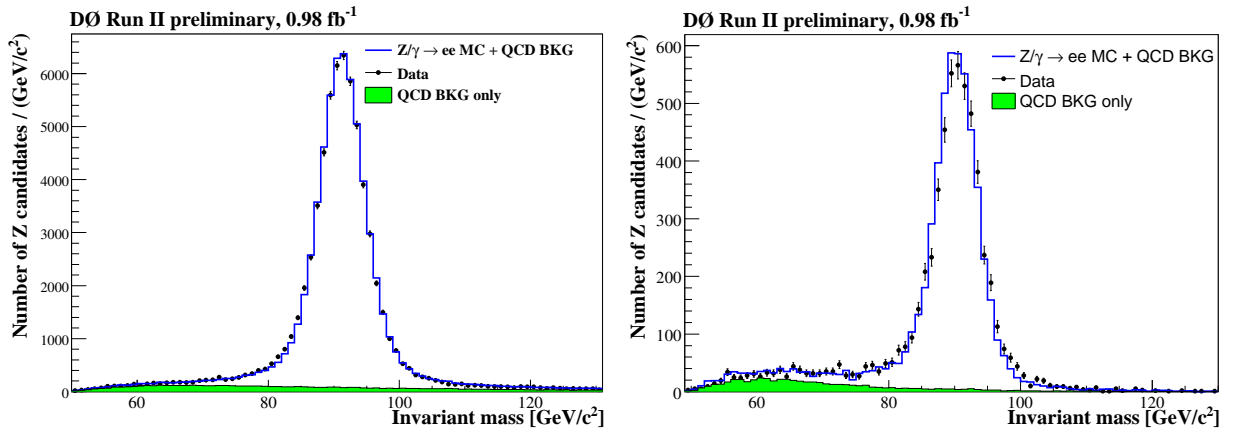


FIG. 1: Comparisons of data and Monte Carlo + background. On the left is the invariant mass distribution for the inclusive sample and on the right is the invariant mass distribution for events containing a Z boson with $|y| > 2$. Uncertainties on the data points are statistical. The χ^2 per degree of freedom between the simulation and data is 102/80 for the inclusive distribution and 112/80 for the subset of the data with $|y| > 2$.

the EM candidates must pass the online trigger requirements. The electron candidates are further required to have transverse momentum $p_T > 25$ GeV/ c . The invariant mass of the electrons should be consistent with that of the Z boson ($70 < M(ee) < 110$ GeV/ c^2). If the event has both its candidate electrons in the central calorimeter (CCCC events), both electrons are required to have a track extrapolated from the same vertex through the central tracking system to the center of the calorimeter cluster within resolutions. Because the tracking efficiency decreases with rapidity in the endcap region, events with an endcap calorimeter electron candidate (CCEC and ECEC events) are only required to have one electron with a matching track. After these requirements, 23,959 CCCC, 30,344 CCEC, and 9,598 ECEC events are selected, 5,412 of them have a Z boson with $|y| > 2$.

III. ANALYSIS PROCEDURE

Electron identification efficiencies are measured using a combination of data and a GEANT-based [15] simulation of the DØ detector. The average electron identification efficiencies are measured from Z events, and are parameterized in terms of the electron transverse energy and, for some variables, the vertex position along the beam axis or electron incident angle. The dependence of the overall selection efficiency on the Z boson q_T is parameterized from the GEANT simulation. A measurement of this shape from the data agrees well with the simulation within statistical uncertainties.

The dominant backgrounds are from photon plus jet events and di-jet events, with photon and jets misidentified as electrons. The kinematic properties of these events are obtained from events that pass most of the Z selection criteria, but fail some electron identification requirements. The shapes of the kinematic distributions from these samples depend only weakly on what selections are used. The size of the background is obtained by fitting the invariant mass distribution of the data sample to a sum of a signal shape obtained from a parameterized simulation of the detector response and the invariant mass distribution from the background sample. The background fractions are $1.30 \pm 0.14\%$, $8.55 \pm 0.26\%$, and $4.71 \pm 0.30\%$ for CCCC, CCEC, and ECEC events respectively. The dijet sample is used to parameterize the shape of the background distribution as a function of q_T , and a systematic uncertainty is assigned by varying the background sample. Figure 1 shows the data/simulation comparison for the Z/γ^* invariant mass distribution. The simulation plus background model reproduces the measured invariant mass distribution well for both the inclusive sample, and for a restricted sample of events at large boson rapidity.

The data are corrected for acceptances within a generator-mass range of 40 to 200 GeV/ c^2 , and for selection efficiencies using a parameterized simulation. We use ResBos [5] as the event generator which does the resummation calculation in the b -space using the Ladinsky-Yuan parameterization for low q_T and a NLO pQCD calculation for high q_T , we use PHOTOS [16] to simulate the effects of final state photon radiation. The overall acceptance \times efficiency falls slowly from a value of 0.27 at low q_T to a minimum of 0.19 at $q_T = 40$ GeV/ c , and slowly increases for large q_T . The spectrum is further corrected for detector resolution effects using RUN (Regularized Unfolding) [17] to obtain the true differential cross section $d\sigma/dq_T$.

The uncertainties on the unfolded Z boson p_T spectrum arise from uncertainties on the electron energy calibration, the electron energy resolution, and the effect of parton distribution functions on the acceptance. The uncertainties

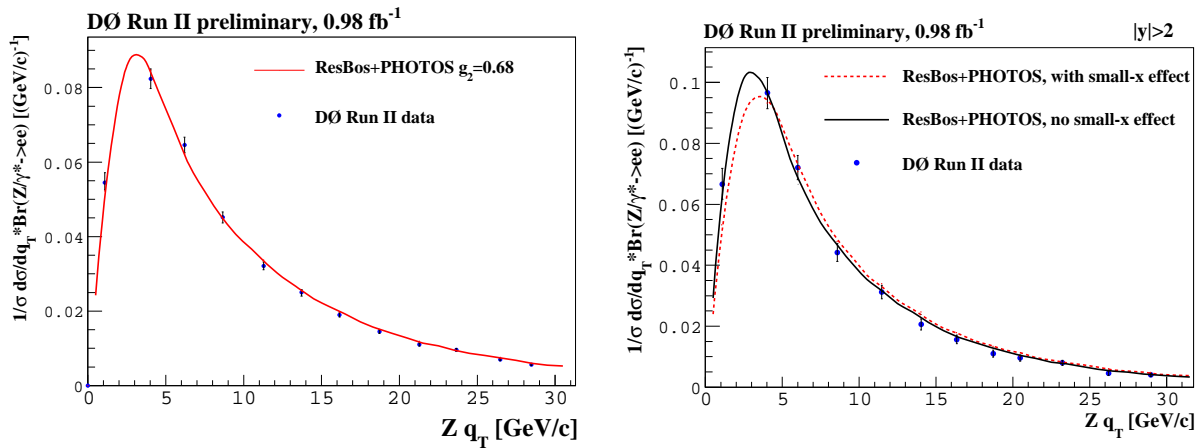


FIG. 2: $\frac{1}{\sigma} \frac{d\sigma}{dq_T}$ for the inclusive sample (left) and the sample with Z boson $|y| > 2$ (right) with $q_T < 30$ GeV/ c . The points are the data. The solid curve is from a theoretical calculation using ResBos [5]. For events with $|y| > 2$, also shown as dashed line is the prediction from the form factor modified after studies of small- x DIS data [9]. The default values for the parameters g_1 , g_2 and g_3 [6] are used in the theoretical calculations. The χ^2 per degree of freedom between the data and the model is 12/11 for the inclusive sample, 11/11 and 32/11 for the model without and with small- x effect for the sample with Z boson $|y| > 2$.

on the unfolded spectrum are estimated by observing the change when the smearing parameters are varied within their uncertainties. CTEQ 6.1m was used as the default parton distribution function (PDF), uncertainties due to the PDF's are estimated using the procedure described in [18].

IV. RESULTS

The final result in the Z boson $q_T < 30$ GeV/ c range, with statistical and systematic uncertainties added in quadrature, is shown in Figure 2 for the inclusive sample and for the sample with $|y| > 2$. For the theoretical calculation, we use ResBos with published values of the non-perturbative parameters [6]. Good agreement between data and ResBos prediction is observed for all rapidity ranges, which indicates the b -space resummation calculation introduced by Ladinsky-Yuan works well for the low q_T region.

Z boson events produced at large rapidities ($|y| > 2$) are also used to test the small- x prediction. We compare data with the theoretical prediction with the form factor as modified after studies of small- x DIS data [9]. The default values for the parameters g_1 , g_2 , and g_3 [6] obtained from large- x data are used. The χ^2 per degree of freedom for the data to the ResBos calculation using the default parameters is 11/11, while that for the modified calculation is 32/11, corresponding to a probability of 0.1%. The data in the $|y| > 2$ region prefer the unmodified calculation. It remains to be seen if retuning of the non-perturbative parameters could improve the agreement for the modified calculations.

Figure 3 shows the measured differential cross section in the range $0 < q_T < 260$ GeV/ c compared to the ResBos calculation with its default parameters [6] and to a pQCD calculation at NNLO [2]. The agreement between data and ResBos is good for q_T 's less than about 30 GeV/ c . At higher q_T 's, the data agree better with the NNLO calculation than with Resbos, which uses a NLO pQCD calculation for these q_T values.

Table I summarizes the measurements. Figure 4 provides a breakdown of the experimental uncertainties. The largest uncertainty is the dependence of the lepton isolation efficiencies on the boson q_T . Systematic uncertainties, especially those due to detector resolution, are correlated between q_T bins. Table II provides a description of this effect in the form of a correlation matrix.

The ResBos prediction describes the data well for $q_T < 30$ GeV/ c but underestimates the cross section at high q_T . The NNLO predictions describes the data well for $q_T > 30$ GeV/ c region. The CSS model parameter most sensitive to the shape at small q_T is called g_2 by the ResBos authors. In the fit, we fix other phenomenological parameters to the values obtained in [6] and only vary the value of g_2 . A minimum χ^2 of 9 for 11 degrees of freedom between the model and the data for $q_T < 30$ GeV/ c is found when $g_2 = 0.77 \pm 0.06$ GeV 2 .

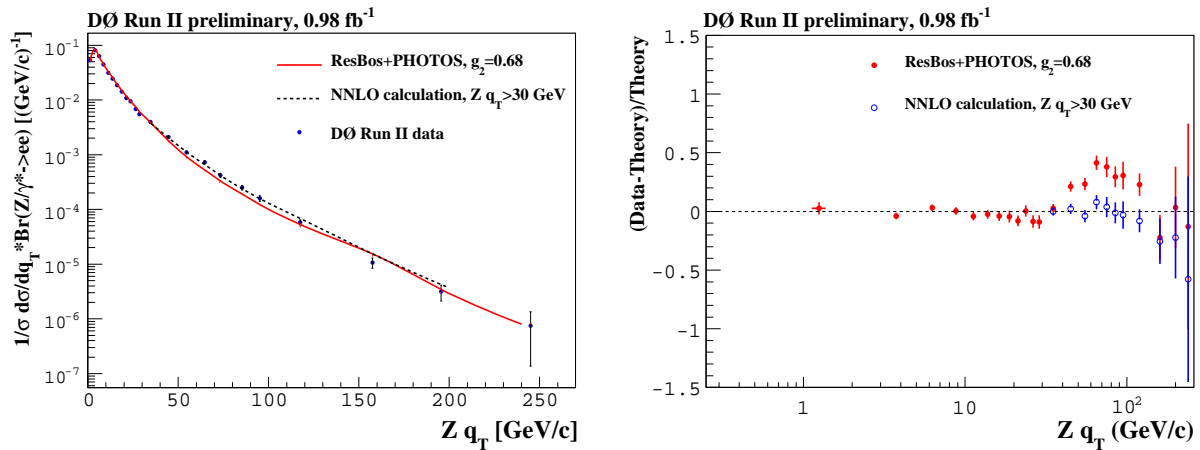


FIG. 3: The differential cross section as a function of q_T compared to the theoretical calculations for the entire range measured (left) and the fractional differences between data and the theoretical predictions (right).

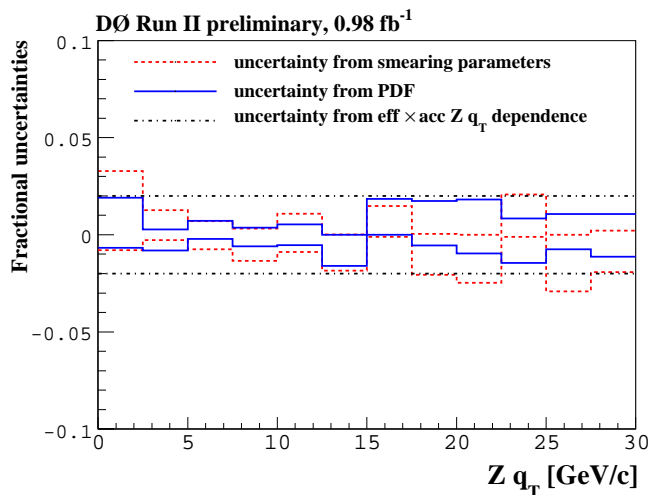


FIG. 4: Fractional systematic uncertainty as a function of Z boson q_T due to uncertainties in the calorimeter resolutions (dashed), parton distribution functions (solid), and dependence of the acceptance \times efficiency on the boson q_T (dot).

V. CONCLUSIONS

In conclusion, we have measured the differential spectrum $\frac{1}{\sigma} \frac{d\sigma}{dq_T}$ for Z boson events produced in $p\bar{p}$ collisions at a center-of-mass energy of 1.96 TeV for boson transverse momenta in the range $0 < q_T < 260 \text{ GeV}/c$ and Z rapidities $|y| < 3$. The overall uncertainty of this measurement has been reduced compared with the previous measurements. We find that for $q_T < 30 \text{ GeV}/c$, the CSS resummation model used in ResBos describes the data very well at all rapidities. Using Ladinsky-Yuan's parameterization, we obtain $g_2 = 0.77 \pm 0.06 \text{ GeV}^2$. Our data at $q_T > 30 \text{ GeV}/c$ agree well with predictions of NNLO QCD, while the prediction from the NLO calculation used by ResBos for these large q_T values is a little bit low. Our data with $|y| > 2$ disfavors a variant of this model that incorporates an additional small x form factor when a tune for g_1 , g_2 , and g_3 from large- x data is used.

Acknowledgments

We thank the staffs at Fermilab and collaborating institutions, and acknowledge support from the DOE and NSF (USA); CEA and CNRS/IN2P3 (France); FASI, Rosatom and RFBR (Russia); CAPES, CNPq, FAPERJ, FAPESP and FUNDUNESP (Brazil); DAE and DST (India); Colciencias (Colombia); CONACyT (Mexico); KRF and KOSEF (Korea); CONICET and UBACyT (Argentina); FOM (The Netherlands); Science and Technology Facilities

q_T bin (GeV/c)	average q_T	$\frac{1}{\sigma} \frac{d\sigma}{dq_T}$ (GeV $^{-1}$)	σ (stat.)	σ (syst.)
0-2.5	1.09	0.0532	0.0013	0.0024
2.5-5.	4.03	0.0808	0.0012	0.0019
5.0-7.5	6.22	0.0633	0.0011	0.0014
7.5-10.0	8.66	0.0443	0.0009	0.0011
10.0-12.5	11.28	0.0315	0.0008	0.0008
12.5-15.0	13.72	0.0246	0.0007	0.0006
15.0-17.5	16.16	0.0186	0.0006	0.0005
17.5-20.0	18.72	0.0142	0.0005	0.0005
20.0-22.5	21.28	0.0109	0.0004	0.0003
22.5-25.0	23.66	0.0094	0.0004	0.0002
25.0-27.5	26.37	0.0069	0.0003	0.0002
27.5-30.0	28.47	0.0055	0.0003	0.0001
30.0-40.0	34.63	0.0039	0.0001	0.0001
40.0-50.0	44.63	0.0021	0.00007	0.00006
50.0-60.0	54.63	0.0011	0.00005	0.00003
60.0-70.0	64.63	0.00073	0.00004	0.00002
70.0-80.0	73.38	0.00042	0.00003	0.00002
80.0-90.0	85.38	0.00025	0.00002	0.00001
90.0-100.0	95.13	0.00016	0.000017	0.000008
100.0-140.0	117.50	0.00006	0.000005	0.000003
140.0-180.0	157.50	0.000011	0.000002	0.0000007
180.0-220.0	195.50	0.000003	0.000001	0.0000003
220.0-260.0	245.50	0.00000071	0.00000061	0.00000006

TABLE I: The differential cross section $\frac{1}{\sigma} \frac{d\sigma}{dq_T}$ for Z/γ^* events produced with mass between $40 < M_{ee} < 200$ GeV/c 2 in bins of q_T with statistical and systematic uncertainties.

bin	1	2	3	4	5	6	7	8	9	10	11	12
1	1	-0.38	0.08	-0.01	0	0	0	0	0	0	0	0
2	-0.38	1	-0.47	0.15	-0.05	0.02	-0.01	0	0	0	0	0
3	0.08	-0.47	1	-0.43	0.12	-0.04	0.01	0	0	0	0	0
4	-0.01	0.15	-0.43	1	-0.40	0.09	-0.01	-0.01	0.01	0	0	0
5	0	-0.05	0.12	-0.40	1	-0.36	0.04	0.03	-0.02	0.01	-0.01	0
6	0	0.02	-0.04	0.09	-0.36	1	-0.33	-0.01	0.06	-0.04	0.02	0
7	0	-0.01	0.01	-0.01	0.04	-0.33	1	-0.28	-0.07	0.10	-0.05	0.01
8	0	0	0	-0.01	0.03	-0.01	-0.28	1	-0.23	-0.15	0.13	-0.05
9	0	0	0	0.01	-0.02	0.06	-0.07	-0.23	1	-0.14	-0.21	0.15
10	0	0	0	0	0.01	-0.04	0.10	-0.15	-0.14	1	-0.12	-0.28
11	0	0	0	0	-0.01	0.02	-0.05	0.13	-0.21	-0.12	1	-0.03
12	0	0	0	0	0	0	0.01	-0.05	0.15	-0.28	-0.03	1

TABLE II: The correlation matrix for the differential cross section given for the first 12 bins ($q_T < 30$ GeV/c) of Table I.

Council (United Kingdom); MSMT and GACR (Czech Republic); CRC Program, CFI, NSERC and WestGrid Project (Canada); BMBF and DFG (Germany); SFI (Ireland); The Swedish Research Council (Sweden); CAS and CNSF (China); Alexander von Humboldt Foundation; and the Marie Curie Program.

-
- [1] P.B. Arnold and M.H. Reno, Nucl. Phys. **B319**, 37 (1989); R.J. Gonsalves, J. Pawlowski, and C-F. Wai, Phys. Rev.D **40**, 2245 (1989).
[2] K. Melnikov, F. Petriello, Phys. Rev. D **74**, 114017 (2006).
[3] J. Collins, D. Soper, G. Sterman, Nucl. Phys. **B250** (1985) 199.
[4] P. B. Arnold and R. Kauffman, Nucl. Phys. **B349**, 381 (1991).
[5] C. Balazs, C.P. Yuan, Phys. Rev. D **56**, 5558 (1997).
[6] F. Landry, R. Brock, P. Nadolsky, C.P. Yuan, Phys. Rev. D **67**, 073016 (2003).
[7] P. Nadolsky, D.R. Stump, and C.P. Yuan, Phys. Rev. D **61**, 014003 (2000) [Erratum-ibid. D **64**, 059903 (2001)].
[8] P.M. Nadolsky, D.R. Stump, and C.P. Yuan, Phys. Rev. D **64**, 114011 (2001).
[9] S. Berge, P. Nadolsky, F. Olness, C.P. Yuan, Phys. Rev. D **72**, 033015 (2005).
[10] CDF Collaboration, T. Affolder *et al.*, Phys. Rev. Lett. **84**, 845 (2000).
[11] DØ Collaboration, B. Abbott *et al.*, Phys. Rev. D **61**, 032004 (2000); DØ Collaboration, B. Abbott *et al.*, Phys. Rev. Lett. **84**, 2792 (2000).
[12] Lei Wang, Ph.D. thesis, University of Maryland (unpublished), FERMILAB-FN-0807-E (2007).
[13] T. Andeen *et al.*, FERMILAB-TM-2365-E (2007).

- [14] DØ Collaboration, V. Abazov *et al.*, “The Upgraded DØ Detector,” Nucl. Instrum. and Methods A **565**, 463-537 (2006).
- [15] R. Brun and F. Carminati, CERN Program Library Long Writeup W5013, 1993 (unpublished).
- [16] E. Barberio and Z. Was, PHOTOS: A Universal Monte Carlo for QED radiative corrections. Version 2.0 Comput. Phys. Commun 79,291 (1994)
- [17] V. Blobel, The RUN manual, Regularized Unfolding for High-Energy Physics Experiments, program manual, unpublished.
- [18] J. Pumplin *et al.*, JHEP **0207** 012 (2002); D. Stump *et al.*, JHEP **0310** 046 (2003).